Observation of low heat capacities for vapor-deposited glasses of indomethacin as determined by AC nanocalorimetry

ARTICLE *in* THE JOURNAL OF CHEMICAL PHYSICS · JULY 2010

Impact Factor: 2.95 · DOI: 10.1063/1.3442416 · Source: PubMed

5 AUTHORS, INCLUDING:

Heiko Huth
University of Rostock
58 PUBLICATIONS **1,438** CITATIONS

SEE PROFILE

Christoph Schick
University of Rostock
418 PUBLICATIONS **6,684** CITATIONS

SEE PROFILE

Observation of low heat capacities for vapor-deposited glasses of indomethacin as determined by AC nanocalorimetry

Kenneth L. Kearns,[#] Katherine R. Whitaker, M. D. Ediger
Department of Chemistry, University of Wisconsin-Madison, Madison, WI 53706 USA

Heiko Huth, Christoph Schick
Institute of Physics, University of Rostock, Rostock 18051 Germany

To be submitted to J. Chem. Phys.

Abstract:

Highly stable glass films of indomethacin IMC with thicknesses ranging from 75 to 2900 nm were prepared by physical vapor deposition. AC nanocalorimetery was used to evaluate the heat capacity and kinetic stability of the glasses as a function of thickness. Glasses deposited at a substrate temperature of 0.84 T_g displayed heat capacities that were approximately 19 J/(mol K) (3 %) lower than glass deposited at T_g (315 K) or the ordinary glass prepared by cooling the liquid. This difference in heat capacity was observed over the entire thickness range and is significantly larger than the ~2 J/(mol K) (0.3 %) difference previously observed between aged and ordinary glasses. The vapor-deposited glasses were isothermally transformed into the supercooled liquid above T_g. Glasses with low heat capacities exhibited high kinetic stability. The transformation time increased by an order of magnitude as the film thickness increased from 75 to 600 nm and was independent of film thickness for the thickest films. We interpret these results to indicate that the transformation of stable glass into supercooled liquid can occur by either a surface-initiated or bulk mechanism. In these experiments, the structural relaxation time of the indomethacin supercooled liquid was observed to be nearly independent of sample thickness.

[#]Current address: Polymers Division, National Institute of Standards and Technology, 100 Bureau Drive, Gaithersburg MD, 20899

Introduction

Physical vapor deposition (PVD) is an important method for producing glasses of organic,[1,2] inorganic,[3,4] and metallic materials.[5,6] PVD often allows the preparation of amorphous samples of materials that tend to crystallize rapidly when cooled as a liquid, e.g., water[7,8] or binary metallic alloys.[6] When used for this purpose, the substrate is held far below the glass transition temperature T_g of the material. The deposition of individual gas phase atoms or molecules onto a substrate allows for the rapid loss of thermal energy and the effective cooling rate can exceed 10^6 K/s. The traditional understanding of PVD is that cooling is so fast that once a molecule hits the substrate surface it has no opportunity to sample different packing arrangements and thus has no opportunity to form a crystal nucleus. For metallic glasses, Turnbull estimated that the substrate temperature must be below 0.25 T_g to avoid crystallization at the surface of the vapor-deposited film.[9] Glasses prepared by vapor deposition onto cold substrates have been found to have high enthalpies, low densities, and low kinetic stabilities.[1,2,10,11] These properties are the natural consequence of glass formation without the optimization of local packing.

We have recently shown that the glasses of two organic molecules (indomethacin and tris-naphthylbenzene) can be readily prepared by PVD at substrate temperatures $T_{substrate}$ ranging from 0.6 T_g up to T_g.[12-14] These materials are "good glass-formers" and they crystallize quite slowly from the liquid state. For such materials, the low $T_{substrate}$ suggested by Turnbull is clearly not required to avoid crystallization. By controlling $T_{substrate}$ to be near 0.85 T_g, glasses having low enthalpy,[12,13,15] high density,[13,14] and high kinetic stability[12-16] have been prepared. These properties have attributed to rapid configurational sampling at the surface of the vapor-deposited

film. This sampling allows optimized local packing at temperatures below T_g. Earlier work also indicated that $T_{substrate}$ could have an important influence on the properties of glasses prepared by physical vapor deposition. For example, Hellman showed that varying $T_{substrate}$ could alter the magnetic anisotropy of Tb-Fe films.[6] Djurisic et al. observed that the lifetimes for amorphous organic light emitting diodes depended upon the substrate deposition temperature.[3]

While traditional calorimetric measurements have been of limited utility for investigating vapor-deposited glasses, the relatively new technique of nanocalorimetry is particularly well-suited. [17-20] Traditional differential scanning calorimetry (DSC) works by heating or cooling a sample while measuring the heat flow, thus allowing the determination of the heat capacity and enthalpy changes. Typically, at least 2 mg of sample material is needed and this is difficult to achieve with PVD if the deposition rate is low. Nanocalorimetry, on the other hand, requires much less material due to the very small thermal mass of the calorimeter. Typically the active area consists of a SiN_x membrane which is only 25 to 1000 nm thick. Since the heat capacity of the calorimeter itself is so small, sub-nanogram samples that are less than 10 nm thick can be investigated with high sensitivity.[17-23]

Here we use AC nanocalorimetry to study the reversing heat capacity C_p of vapor-deposited glasses of indomethacin (IMC). We directly vapor deposit glasses of IMC onto a nanocalorimeter and by appropriately controlling the nanocalorimeter temperature, we can prepare highly stable glasses. AC nanocalorimetry is similar to conventional temperature-modulated DSC techniques in which a small amplitude temperature oscillation is used to separate the reversing and non-reversing components of the heat capacity. For AC

nanocalorimetry, this temperature oscillation results from a small AC voltage that is supplied to a heater integrated onto the nanocalorimeter membrane. The reversing C_p is proportional to the ratio between the amplitudes of the applied heat flow and the resulting temperature oscillation. The temperature change is measured by an integrated thermopile on the nanocalorimeter membrane.

From AC nanocalorimetry we observe that the reversing C_p of the as-deposited stable glass is about 3% lower than that obtained for the IMC glasses prepared by cooling the liquid. Although previous work has shown that aging a glass can lower C_p,[24-27] the change observed here is much larger than any previously reported. This is consistent with the view that vapor-deposition can prepare glasses that are similar to those that would be obtained by aging an ordinary glass for thousands of years or more.[13,15] Due to the relatively large difference in C_p and the high sensitivity of nanocalorimetry, we can follow the isothermal transformation of the stable glass into the supercooled liquid by measuring C_p. As we have reported elsewhere in a preliminary account,[28] the transformation time increases linearly with film thickness between 75 and 600 nm while thicker films do not show a dependence upon sample size. These results are interpreted in terms of two parallel transformation mechanisms. Finally, the structural relaxation time τ_α of the IMC supercooled liquid, as determined by AC nanocalorimetry, is shown to be consistent with previous dielectric work[29,30] and nearly independent of sample thickness.

Experimental methods

Materials. Indomethacin (IMC) was purchased as the γ crystalline polymorph from Sigma (St. Louis, MO) and used without further purification. The chemical purity was greater than 99%. The melting temperature of the as-received material was previously determined (T_m = 432.8 K) and agreed with literature data for the γ polymorph to within 1 K.[12]

Vapor deposition. IMC films of various thicknesses were prepared by physical vapor deposition. Crystalline IMC was placed in a quartz crucible, heated, and deposited onto nanocalorimeters fabricated by Xensor Integration (XEN-39321). The deposition rate was controlled by the amount of heat supplied to the crucible. The rate was maintained at 0.20 ± 0.03 nm/s for all the films prepared for this study, as measured by a quartz crystal microbalance QCM (Sycon). The QCM was also used to determine the final thickness of the samples. The absolute thickness was within 10% of the measured value for films less than 1 μm thick as determined by comparisons with separate x-ray reflectivity[13] and ellipsometry experiments for films deposited under the same conditions. A copper stage was used to hold the nanocalorimeters in the deposition chamber and maintain the temperature during deposition. The temperature of the copper stage was controlled by a Lakeshore 340 controller and measured with 4-wire RTD sensors (Omega). The pressure inside the chamber was ~ $5x10^{-8}$ torr prior to and during the deposition.

AC nanocalorimetry. AC nanocalorimetry was performed outside of the deposition chamber in an apparatus similar to that described previously.[18,23] Only a brief description of the apparatus will be given here. Each nanocalorimeter consists of a micromachined SiN_x membrane with an

integrated heater and an integrated thermopile. A reference and a sample nanocalorimeter were utilized in a differential measurement scheme. A small temperature oscillation on both nanocalorimeter membranes results from an AC voltage supplied to the heaters by a lock-in amplifier (Signal Recovery, model 7265). The amplitude of the temperature modulation can be measured by an integrated thermopile on the nanocalorimeter chip. The reversing heat capacity C_p of the IMC film is directly proportional to the difference in the temperature amplitude on reference and sample nanocalorimeters. The differential setup allows for sensitivity in the pJ/K range.[18] The amplitude and frequency of the temperature oscillation are controlled by the voltage supplied from the lock-in amplifier. Unless otherwise stated, for the experiments reported here the frequency of the temperature modulation was 20 Hz with an amplitude of ~0.25 K. All nanocalorimetry experiments were conducted under dry nitrogen.

The sample and reference nanocalorimeters were placed in a temperature-controlled housing to allow temperature jumps and linear heating/cooling ramps while maintaining the two nanocalorimeters at the same temperature. Absolute temperature was calibrated using the liquid crystal 4'-(octyloxy)-4-biphenylcarbonitrile; the housing temperature is known to within ±1 K.

For the experiments reported here, we typically used the following temperature program. After loading the sample nanocalorimeter into the housing, the temperature of the housing was ramped to the annealing temperature T_{anneal} at a rate of ~5 K/min. The housing temperature was then held isothermally until the as-deposited sample transformed into the supercooled liquid. At this point, the housing temperature was lowered to room temperature and then ramped several times between room temperature and ~ 350 K at heating/cooling rates of ±1 K/min. (Below 310 K,

the cooling rate decreased due to the lack of active cooling of the housing.) The reversing heat capacity C_p was measured throughout this entire temperature program. Thus the isothermal annealing step is actually quasi-isothermal for the sample since the nanocalorimeter temperature is being slightly modulated at all times.

Results

Reversing C_p of supercooled liquid. Although the most important aspect of this paper is the behavior of the as-deposited glasses, to provide context we begin with results on the supercooled liquid that is obtained after annealing the as-deposited glasses. Figure 1 shows the reversing heat capacity C_p (at 20 Hz) for a 600 nm IMC film obtained using nanocalorimetry (solid line). For reference, specific reversing heat capacity values c_p (at 0.0167 Hz) are also shown for a bulk sample of IMC; this data was obtained using quasi-isothermal temperature modulated DSC (qi-TMDSC) and is reproduced from reference 16.

A gradual rise in the reversing heat capacity is observed for both techniques upon increasing the temperature. At low temperatures, the IMC molecules are immobile on the timescale of the temperature oscillation; the heat that is supplied to the sample only goes into increasing the amplitude of the vibrational motion in the system. At temperatures well above T_g, IMC molecules rearrange rapidly compared to the timescale of the temperature oscillation. The heat capacity in this temperature regime is greater because increasing temperature requires energy to increase the amplitude of vibrational motion as well as energy to change the structure of the liquid. Since the frequency of the nanocalorimetry experiment (20 Hz) is much higher than the

qi-TMDSC experiment (0.0167 Hz), the transition between these two regimes is shifted to higher temperature. The observed 14 K shift between the two curves is consistent with the observed temperature dependence of the dielectric relaxation time[29,30] for IMC. Across this same temperature interval, the dielectric relaxation time shifts by 2.9 decades, in good agreement with the 3.1 decade difference between the measurement frequencies of the two calorimetry techniques.

The behavior shown in Figure 1 is sometimes described as the "dynamic glass transition.[31]" The transition temperatures shown in the figure should not be confused with the T_g determined from differential scanning calorimetry (DSC). When "T_g" is used in this paper, we refer to the onset temperature observed in a DSC experiment upon heating an IMC glass that has been prepared by first cooling the supercooled liquid at 10 K/min and then promptly reheating at 10 K/min. For IMC, the T_g determined in this manner is 315 K.

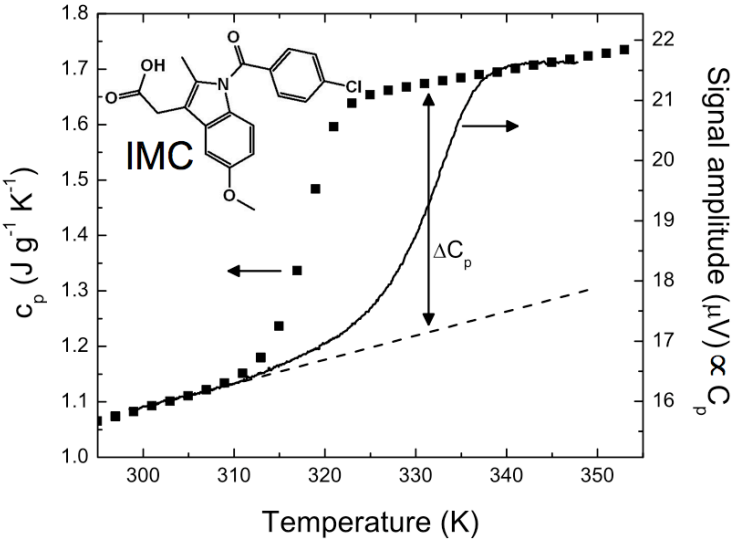

Figure 1: Reversing heat capacity of indomethacin measured by conventional and nano-scale calorimetry. Conventional calorimetry (black squares, left axis) was performed on ~10 mg of sample using quasi-isothermal experiments while nanocalorimetry (solid line, right axis) data was obtained for a 600 nm film during slow temperature scanning. The temperature shift

between the two data sets is expected given the difference in frequency (0.0167 Hz vs. 20 Hz) for the two measurements. The dashed line is a linear extrapolation of the glass heat capacity response. ΔC_p is defined at the midpoint of the C_p curve as indicated. The right axis was scaled to superpose the two data sets at low and high temperature because the AC calorimetry technique does not easily provide absolute values for specific heat capacity. Inset: Structure of IMC.

Figure 2 shows the amplitude of the heat capacity step ΔC_p observed for the supercooled liquid of IMC in nanocalorimetry experiments on films of varying thickness. ΔC_p is defined in Figure 1 and measured in units of μV; this voltage is the amplitude of the differential response of the thermopiles on the sample and the reference nanocalorimeters. In the limit of thin films and constant power, the observed signal amplitude is proportional to the sample heat capacity C_s. This proportionality is valid in the limit $C_S/C_0 << 1$ where C_0 is the heat capacity of the empty nanocalorimeter sensor. The red line in Figure 2 shows that this thin film approximation adequately describes our data for films thinner than 300 nm. For thicker samples, the condition $C_S/C_0 << 1$ is no longer valid. Under these conditions, the observed signal amplitude (and the amplitude of ΔC_p) is expected to be proportional to

$$\frac{1}{C_0} - \frac{1}{C_0 + C_S}. \qquad (1)$$

The black curve shows that the experimental data is well described by this equation. For these calculations, we modeled the nanocalorimetry membrane as 1 μm of SiN_x; we neglected all other materials and the surrounding N_2 gas. For SiN_x, we used c_p =0.4 J/(g K) and ρ=3.4 g/cm^3 (data from reference 32). For IMC, we used c_p = 1.5 J/(g K) and ρ =1.31 g/cm^3. The vertical dashed line in Figure 2 indicates $C_s = C_0$. In this case the measured step in the signal amplitude is half of the value expected from the thin film approximation.

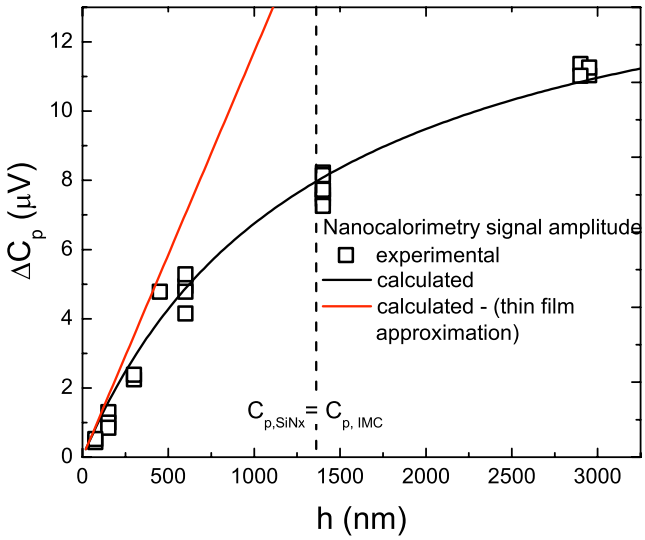

Figure 2: Thickness dependence of the observed ΔC_p for IMC films. For thin films, the observed ΔC_p increases linearly as expected. As the heat capacity of the sample becomes comparable to that of the membrane (vertical dashed line), a non-linear relationship is observed; this relation is correctly described by equation 1.

Reversing C_p of as-deposited glasses. Figure 3 shows the influence of the substrate temperature during deposition ($T_{substrate}$) on the reversing C_p of as-deposited IMC glasses. Figure 3A shows results for a 350 nm film deposited at $T_{substrate} = T_g = 315$ K (where T_g is defined by DSC as discussed above). The temperature program used to obtain this data was comprised of four steps. First, the as-deposited IMC glass was heated at 1 K/min from room temperature to 325 K. Next, the sample was held at 325 K (T_g + 10 K) for at least 3600 seconds to assure that all memory of the deposition process had been erased. Third, the sample was cooled to 300 K at ~1 K/min. Finally, the sample was heated again (Figure 3A, gray line) through the dynamic glass transition at 1 K/min.

Figure 3A shows that C_p values obtained during the first and second heating scans of the sample vapor-deposited at 315 K lie on top of one another. We interpret this result to indicate that this

vapor deposition prepared a glass similar to the one obtained by cooling the supercooled liquid. This is the expected result. It has been previously shown that depositions with $T_{substrate} \approx T_g$ prepare glasses with the enthalpy and kinetic stability of the ordinary glass prepared by cooling the supercooled liquid.[12-14]

In contrast, Figure 3B show that C_p for IMC vapor-deposited with $T_{substrate}$ = 265 K (0.84 T_g) is measurably lower than C_p for the same sample after thermal cycling. The temperature-time profile used to obtain this data is similar to the one described above except that the first heating was performed at ~5 K/min and the isothermal hold done at 320 K lasted 20,000 seconds. The vertical line at 320 K indicates the increase in C_p that occurred during annealing. The similarity between the heating and cooling scans for the post-anneal sample indicates that the long isothermal anneal at 320 K erased the thermal history associated with the deposition process. Previous work has shown that glasses vapor-deposited near 0.85 T_g have lower enthalpy,[12,13,15] higher resistivity to water uptake,[33] higher density,[13,14] and higher mechanical moduli[34] than ordinary glasses. While a difference in C_p might have been anticipated given this, the 3% difference shown in Figure 3B is unprecedented and will be discussed below.

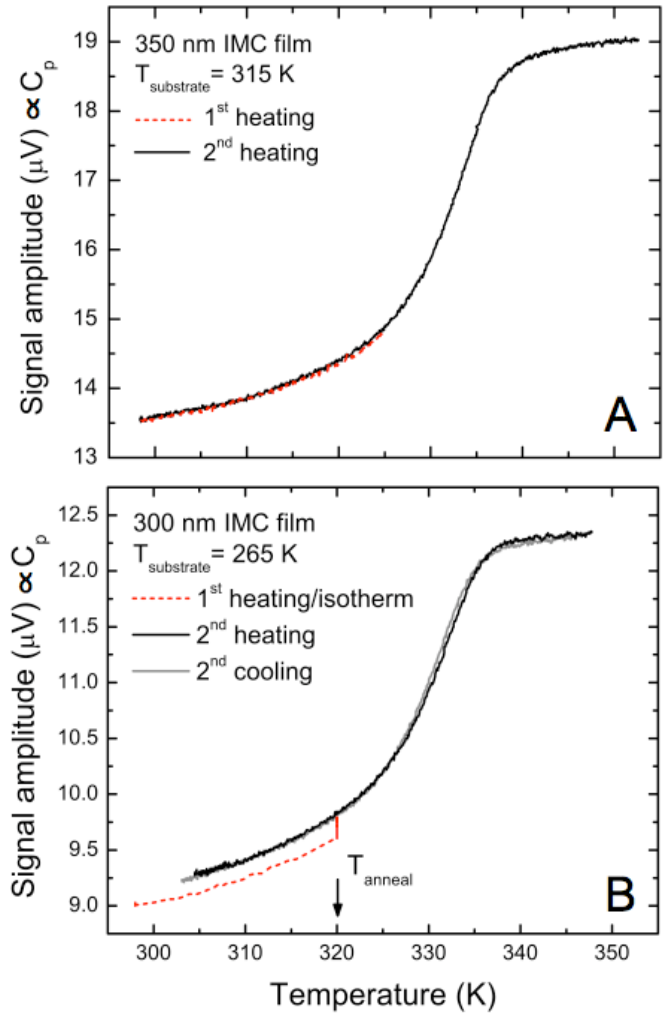

Figure 3: Effect of $T_{substrate}$ on the C_p of IMC glasses deposited at 0.2 nm/s. A) Reversing C_p for 350 nm thick IMC film deposited at $T_{substrate}$ = 315 K. The C_p of the as-deposited sample (black line) matches that observed after temperature cycling (gray line). B) Reversing C_p for 300 nm thick IMC film deposited at $T_{substrate}$ = 265 K. The C_p of the as-deposited sample (red line) is lower than the post-anneal samples (black and gray). The similarity between the heating (black) and cooling (gray) curves signifies the erasure of the thermal history associated with the deposition process.

Figure 4 quantifies the heat capacity of as-deposited IMC glasses ($T_{substrate}$ = 265 K) as a function of sample thickness. Because the signal in our differential measurements is not proportional to the sample C_p when comparing samples of different thicknesses (see Figure 2), we normalize results for each sample to ΔC_p for that sample after temperature cycling. The inset of Figure 4

graphically describes the manner in which this calculation is done; linear extrapolations of C_p for the ordinary and as-deposited glass are extended to high temperatures and the supercooled liquid data is extrapolated to low temperatures. The ratio between ΔC_p for the as-deposited stable glass (SG) and thermally cycled ordinary glass (OG) is plotted in the main figure.

Figure 4 shows that C_p for IMC glasses vapor-deposited at 265 K is lower than thermally cycled samples by an amount equal to ~12% of ΔC_p(OG). Within the scatter of the data, this difference is independent of film thickness. From the data shown in Figure 1 and the molar mass of IMC (357.8 g/mol), it follows that the change in molar heat capacity ΔC_m(OG) for IMC is 160 J/(mol K). We assume that this same result applies to IMC films as thin as 75 nm. Thus we estimate the as-deposited IMC glasses have C_m values that are 19 ± 10 J/(mol K) lower than the ordinary glass. The large error bar reflects the variability from run-to-run for the measured difference in glassy C_p between the ordinary and stable glass.

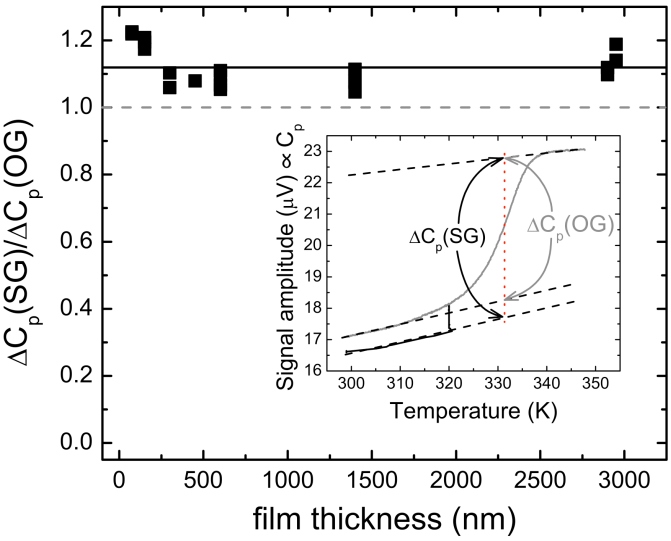

Figure 4: The ratio of ΔC_p for the as-deposited stable IMC glasses (black squares) as compared to the post-anneal ordinary glass (dashed gray line) as a function of thickness. Each of the as-deposited glasses was deposited at 0.2 nm/s with $T_{substrate}$ = 265 K. The solid horizontal black line is a line of best fit with the slope constrained to zero. Inset: Definitions of ΔC_p(SG) and

ΔC_p(OG). The position of the dotted vertical line is determined from the half-height of ΔC_p(OG).

Kinetics of stable glass transformation. Figure 5 illustrates the isothermal transformation kinetics of stable IMC films of different thicknesses and shows that thicker films require more time to complete the transformation. The vertical axis presents ϕ_{SG}, which is the fraction of the sample responding with the heat capacity of the stable glass. ϕ_{SG} is determined from the C_p increase observed during isothermal annealing of the stable glass, as shown in Figure 3B. ϕ_{SG} is linearly related to the C_p change and defined to equal 1 at t=0. When the transformation to the supercooled liquid is complete, ϕ_{SG} is equal to 0. As other experiments have shown that the transformation from the stable glass is heterogeneous,[35,36] it is reasonable to interpret the change in C_p in this manner, i.e., a ϕ_{SG} of 0.5 means that half of the sample is unchanged from its initial stable glass state and half the sample is the equilibrium supercooled liquid.

The shape of the curves shown in Figure 5 changes significantly with film thickness. For the 150 and 600 nm thick films, ϕ_{SG} decreases almost linearly beginning at t = 0. For these films, $\phi_{SG} = 0$ is defined when an abrupt change in slope is observed. The slight decrease of ϕ_{SG} to negative values is attributed to instrument drift. Drifts of similar magnitude have been observed when two empty nanocalorimeters are used; the effect of drift is exacerbated for the thinnest films. An unexpected $\phi_{SG}(t)$ profile is observed for the 2900 nm thick films. At short times, ϕ_{SG} decreases slowly, as expected. After about 10000 seconds, ϕ_{SG} begins to increase again. Given our interpretation of the data, this would naively indicate that some fraction of the supercooled liquid is transforming back into the stable glass. Since this interpretation is unphysical, several

control experiments were performed on 2900 nm films to test whether the observed maximum might be an experimental artifact.

The data in Figure 5 shows that the maximum in the $\phi_{SG}(t)$ is observed at two distinct frequencies. For the experiment shown, the oscillation frequency was switched back and forth between 20 and 200 Hz during the isothermal anneal. Within experimental noise, no discernable change in the transformation curve is observed.

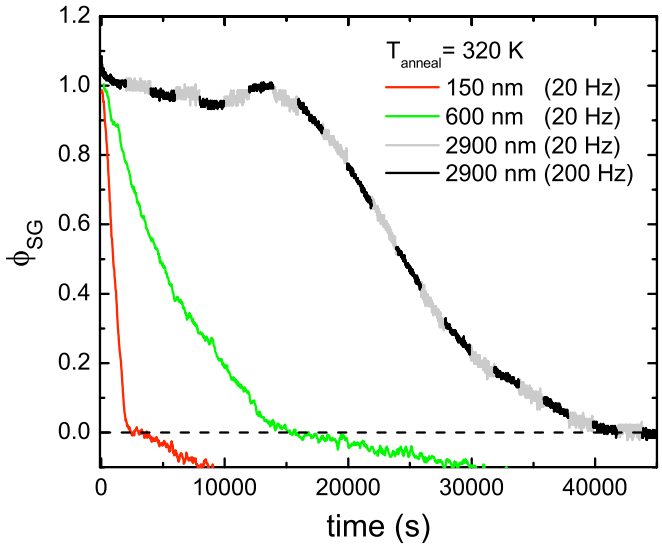

Figure 5: Fraction of sample that is a stable glass ϕ_{SG} as a function of time for IMC films of three different thicknesses. The annealing temperature T_{anneal} was 320 K for all three experiments. The temperature oscillation frequency f was held constant at 20 Hz for the 150 nm and 600 nm thick films. For the 2900 nm sample, f was switched back and forth between 20 and 200 Hz as indicated.

Figure 6 shows that changing T_{anneal} does not modify the shape of $\phi_{SG}(t)$ for the 2900 nm thick films. As T_{anneal} is decreased from 325 K down to 318 K, the total transformation time increases as expected, but the increase in ϕ_{SG} at intermediate times remains in all four curves. For T_{anneal} = 325 K, we halved the amplitude of the temperature oscillation (black curve). This data and that

obtained at an annealing temperature of 324 K (with the normal temperature oscillation amplitude) decay very similarly as expected.

Based on these tests, we conclude that the maximum observed in $\phi_{SG}(t)$ for films of 2900 nm is not an experimental artifact. We do not yet understand its origin. We are hopeful that coordinated experiments with other techniques, such as ellipsometry, will be fruitful.

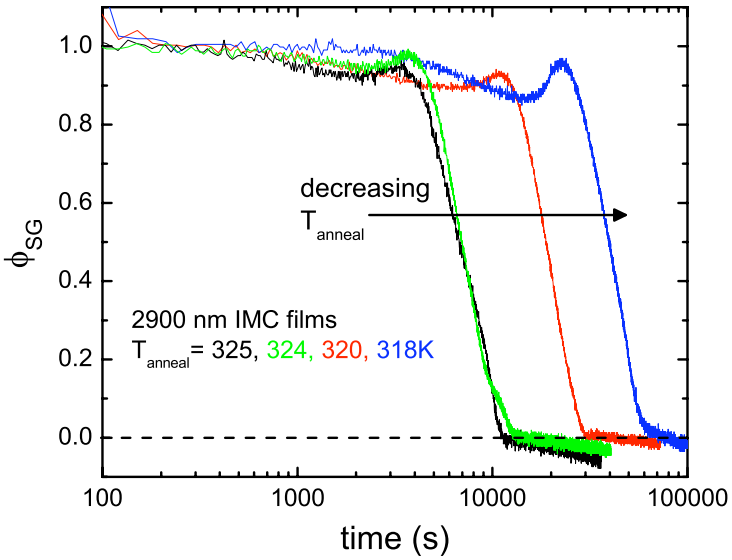

Figure 6: Fraction of the sample that is a stable glass ϕ_{SG} as a function of time for four different annealing temperatures T_{anneal}. The film thickness was 2900 nm for each of these experiments. The amplitude of the temperature oscillation was halved to ~0.13 K for T_{anneal} = 325 K.

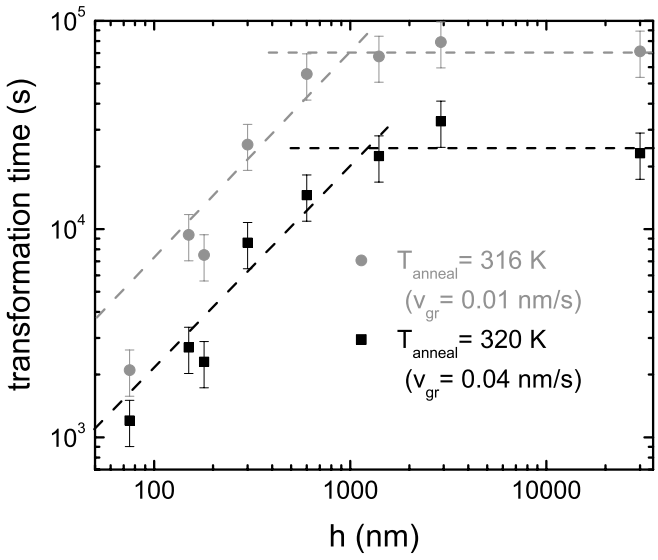

Figure 7: Thickness dependence of the time required to transform the stable glass into the supercooled liquid. Experiments with T_{anneal} equal to 316 K (gray circles) and 320 K (black squares) are shown. The dashed lines are fits to the transition time data for the 75 nm to 600 nm thickness range and the 1000 nm and greater range. For the thinner regime, the slope is constrained to one, consistent with a surface initiation of a constant-velocity growth front. For the thicker regime, the slope is constrained to zero. The data was obtained using nanocalorimetry in each case except for the ~ 30 μm thick films where qi-TMDSC was used.

Figure 7 shows the total transformation time as a function of film thickness for two different values of T_{anneal}. The transformation time is defined as the time where $\phi_{SG}(t)$ is equal to zero in Figure 5 and 6. Over the entire thickness range, the transformation times increased as T_{anneal} is decreased as expected. For a given T_{anneal}, the transformation times increase with thickness when the film thickness is between 75 and 600 nm. For thicker films transformation times are independent of thickness. As will be described in the Discussion section, we interpret this change in thickness dependence to indicate a change in mechanism. The thin film behavior is consistent with a surface-initiated constant-velocity growth front.[28,35,36] From the data in Figure 7, the velocity of the growth front v_{gr} is calculated to be 0.01 and 0.04 nm/s for T_{anneal} equal to 316 and 320 K, respectively.

Role of dewetting. Optical micrographs of the nanocalorimeters were acquired at various stages during the thermal treatment to ensure that dewetting is not playing any role in the experimental results reported here. Unlike high molecular weight polymer thin films which resist dewetting even above T_g due to intermolecular entanglement,[37] thin films of low molecular weight glass formers have a smaller kinetic barrier to dewetting. Figure 8 shows four micrographs of thermally treated IMC films. We conclude that no dewetting occurred during the isothermal annealing experiments reported in Figures 3, 5, 6, and 7. If a uniform film thickness is to be maintained, the temperature of the IMC film should not be taken above 343 K (T_g+ 28 K) for films thicker than 150 nm.

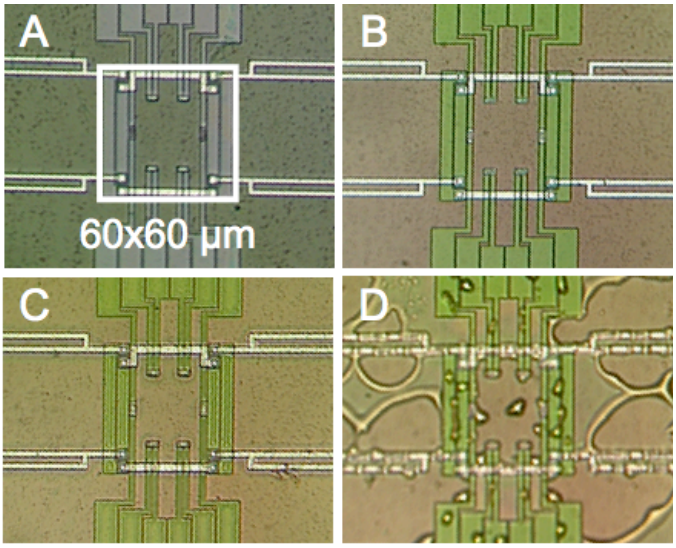

Figure 8: Optical micrographs of the nanocalorimeter surface. In each panel, the horizontal stripes, extending beyond the field of view, are the electrical connections for the heaters. The vertical stripes are electrical connections for the thermopile. A) Cleaned nanocalorimeter prior to deposition. The active area of the calorimeters is 60x60 μm as indicated by the box. B) Nanocalorimeter with 75 nm IMC film after 3600 s of annealing at 318 K. No dewetting is observed. C) Nanocalorimeter with 180 nm film after thermal treatment to 343 K. Again no dewetting is observed. D) Nanocalorimeter with 180 nm film after thermal treatment to 348 K, with indications of dewetting.

Mobility of supercooled IMC as a function of film thickness. Additional nanocalorimetry experiments were performed to measure the temperature dependence of the structural relaxation time τ_α in the thin supercooled liquid IMC samples. These results are shown in Figure 9. After transforming the as-deposited glass into the supercooled liquid by isothermal annealing, we ramped the sample temperature up and down at least six times. For each temperature ramp, we measured the reversing C_p at a different frequency in the range from 20 to 200 Hz. The temperature corresponding with the half height of the rise in C_p is plotted on the x-axis. The structural relaxation time τ_α corresponding to this temperature is plotted on the y-axis; it is determined from the reciprocal of the temperature oscillation frequency f measured in Hz according $\tau_\alpha = 1/ 2\pi f$. For comparison, in Figure 9 we also plot τ_α obtained from dielectric relaxation on bulk IMC samples. A number of previous studies have shown that the frequency dependence of the dynamic glass transition taken from temperature-modulated DSC studies is within about one order of magnitude of the τ_α obtained from dielectric relaxation.[18,23,38] This is also true for IMC, as shown by the similar temperature dependences for the dielectric and nanocalorimetry data in Figure 9. For the case of the dielectric data (both gray and black lines), τ_α was obtained by fitting the Havriliak-Negami function to the dielectric loss. If the dielectric data were analyzed in the same manner as the nanocalorimetry data (i.e., $\tau_\alpha = 1/ 2\pi f_{max}$), those τ_α values would shift down about 0.4 decades, thus making the absolute relaxation times for bulk dielectric measurements quite similar to the nanocalorimetry values obtained on thick films.

Figure 9 indicates that there is little change in τ_α with thickness. Results for the 300 to 2900 nm films coincide with one another to within 2 K. The 150 nm thick film shows a slight shift of about 2.5 K to lower temperatures. The latter effect is just larger than the experimental error

and will be revisited after we improve our method of measuring temperature on the nanocalorimetry membrane. Data for all the films show a temperature dependence similar to the dielectric relaxation data, as expected.

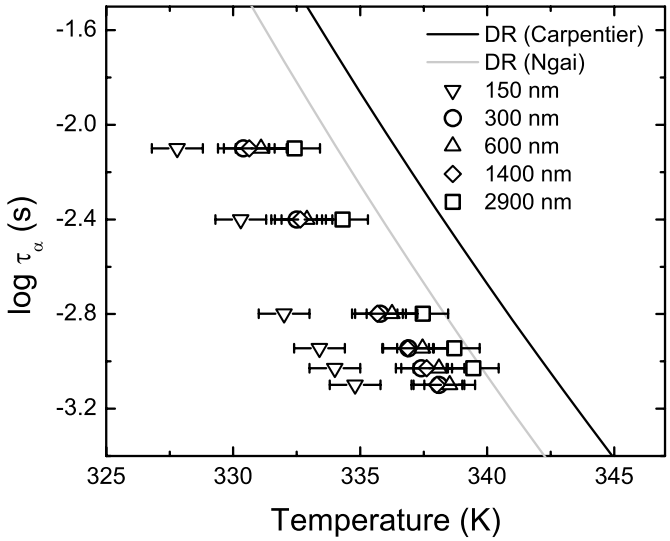

Figure 9: Temperature dependence of the structural relaxation times τ_α from nanocalorimetry data (open symbols) and dielectric relaxation on bulk samples (gray[30] and black[29] lines). The error bars indicate the standard deviation obtained from 3-6 different samples deposited for each thickness.

Discussion

We begin this section by discussing these results in light of the mechanism for stable glass formation. Next, we will discuss the small heat capacity observed for the stable glass within the context of previous aging experiments. We also interpret the thickness-dependent transformation times reported here. Finally, the dependence of τ_α for thin films of IMC will be compared to similar experiments on thin polymer films.

Vapor Deposition: Using surface mobility to prepare stable glasses. A number of previous experiments have demonstrated that dynamics at the surface of a glass can be orders of magnitude faster than in the bulk.[39-43] For IMC at T_g – 20 K, we previously estimated surface mobility is 7 orders of magnitude larger than bulk mobility.[15] Enhanced surface dynamics allows for the formation of stable glasses via physical vapor deposition. Molecules in the liquid-like layer at the surface, estimated to be a few nanometers thick,[13] quickly sample configurations before being buried in the bulk of the film by subsequently deposited molecules. When the substrate temperature is held near T_g, the configurational sampling is fast and nearly complete. Thus vapor-deposition with $T_{substrate}$ equal to T_g is expected to form a supercooled liquid at T_g; when this sample is cooled after deposition, it is nearly equivalent to an ordinary glass formed by cooling the supercooled liquid. In the experiments presented here, this expectation is confirmed by the similar C_p observed for the first and second heating in Figure 3A.

Previous work has shown that vapor deposition onto substrates near 0.85 T_g yields glasses with low enthalpies,[12,13,15] high densities,[13,14] high mechanical moduli,[34] high resistance to vapor

uptake,[33] and high kinetic stabilities.[12-16,34] At 0.85 T_g, surface mobility remains high enough to allow significant configurational sampling. This mobility allows the sample to work its way far down the energy landscape (equivalent to aging an ordinary glass for thousands of years or longer) and the properties listed above are then the natural outcome. Stable glasses have been formed from IMC,[12,13,15,16,33,44] tris-naphthylbenzene,[12-15,35] toluene,[19,45,46] propyl benzene,[46] isopropyl benzene,[46] and ethyl benzene.[46,47] It should be noted that nanocalorimetry techniques were used for characterization in the case of toluene.[19,45]

Low C_p glasses: Aging and physical vapor deposition. Since stable glasses may be regarded as "super-aged", it is natural to compare the properties of stable glasses to previous work on aged glasses. Using adiabatic calorimetry, Bestul and coworkers showed for a number of organic molecules that aging the glass lowers C_p as compared to the ordinary unaged glass.[24-27] This aging also lowers the enthalpy of the glass as assessed by changes in the fictive temperature T_f. T_f is a single-parameter measure of the enthalpy of the glass; lower T_f values indicate lower enthalpy.

Table 1 summarizes the adiabatic calorimetry results of Bestul and coworkers,[24-27] previous calorimetric work on stable glasses of IMC,[15] and the nanocalorimetry work described here. The aging temperature and aging time used by Bestul and coworkers varied from sample to sample. Typically, the aging temperature was around T_g – 10 K and the aging time on the order of several days. As shown in Table 1, the change in fictive temperature between the ordinary and aged samples was only a few K in most cases. The change in molar enthalpy H_m was on the order of a few hundred J/mol while molar heat capacity C_m for the aged glass was roughly 1 J/(mol K)

lower than for the ordinary glass. Among the 4 samples studied by Bestul and coworkers, the changes in H_m and C_m are closely correlated.

In contrast to the results for aged ordinary glasses, much larger effects are observed for vapor-deposited stable glasses of IMC in Table 1. In all cases, the properties of the stable glass correspond to that expected for a super-aged ordinary glass. The fictive temperature is lowered by nearly 30 K and 4000 J/mol differences are observed for H_m.[15] Given the correlation between H_m and C_m for aged samples, the large change in C_m between the ordinary and vapor-deposited IMC is qualitatively reasonable. The magnitude of this C_m difference is comparable to the C_m difference between the ordinary glass and γ crystalline polymorph of IMC (13 J/(mol K)).[48] As shown in Figure 4, low C_p values are consistently observed for IMC vapor-deposited at 0.85 T_g independent of film thickness. The variability shown in Figure 4 leads to the large error bar in Table 1. Although we do not at present understand the origin of this variability, there is no question that stable IMC glasses show a significantly lower C_m than aged ordinary glasses.

Material	**Preparation**	**ΔT_f (K)**	**ΔH_m (J/mol)**	**Change in C_m (J/(mol K))**	**Reference**
o-terphenyl	aging	-2	-172	-0.576	[25]
cis-1,4-polyisoprene	aging	-5	-195	-0.584	[24]
diethyl phthalate	aging	-4.3	-542	-2.429	[27]
selenium	aging	-9	-160	-0.574	[26]
IMC	vapor deposition	-29	-4000 ± 400	-19 ± 10	[12,13,15] and this study

Table 1: Comparison of the changes in fictive temperature T_f, molar enthalpy H_m, and molar heat capacity C_m between an ordinary glass prepared on cooling and glasses prepared either by aging or vapor deposition.

One would, of course, like to understand the molecular origin of the heat capacity difference between the ordinary and vapor-deposited glass. For the crystal and ordinary glass, it is commonly accepted that the heat capacity difference originates from differences in the vibrations of the glass and crystal that result both from the different densities and the disorder of the glass.[49] Further calorimetry experiments on stable and ordinary glasses that extend to lower temperature would be useful. In addition, light scattering and neutron scattering measurements of the vibrational density of states would provide insight into the low heat capacity values observed here for stable glasses.

Transformation of stable glass to supercooled liquid as a function of thickness. The transformation of a glass into a supercooled liquid is usually discussed in terms of a spatially homogeneous picture. As the glass is heated through T_g, all parts of the sample become a supercooled liquid at the same rate. The most commonly used model to describe this transition is that of Tool, Narayanaswamy, and Moynihan (TNM). [50-52] Within the TNM framework, the relaxation time near T_g depends upon both the temperature T and the structure of the material (through the fictive temperature T_f). As neither T nor T_f is spatially varying in the model, the model is a homogeneous description. In this picture, sample size should play no role in the glass as it transforms into the supercooled liquid. Despite being reasonably successful in describing a number of features of organic and inorganic glasses,[53] the TNM model obviously lacks the right form to describe the thickness-dependent transformation of the stable glass shown in Figures 5 and 7.

Recently, it has been shown that stable glasses can transform into supercooled liquids by a surface-initiated process.[28,35,36] For stable glasses of TNB, secondary ion mass spectrometry (SIMS) experiments showed that a growth front, which begins at the free surface, moves through the film at a constant rate.[35] As the front moves through the stable glass film, it leaves supercooled liquid behind it. Such a growth front mechanism provides a natural explanation for how sample thickness can influence the total transformation time of a thin film.

The data for thin films in Figure 7 can be explained by a surface-initiated growth front transformation mechanism. If this mechanism is correct, the total transformation time should scale linearly with film thickness for thin films. This is observed in annealing experiments at both 316 and 320 K. Growth front velocities of 0.04 and 0.01 nm/s for T_{anneal} of 320 and 316 K, respectively, are deduced from fits. These values are in excellent agreement with recent SIMS measurements on IMC stable glasses as a function of annealing time at 319 K; growth front velocities in the range 0.030±0.06 nm/s were reported.[36] Further evidence for the surface-initiated growth front mechanism is found in the shape of the ϕ_{SG} profile for the 150 nm film in Figure 5. This mechanism predicts a linear drop in ϕ_{SG} until 0 is reached and this is a reasonable description of the data. . Very recent work by Leon-Gutierrez et al.[45] on vapor-deposited toluene films is broadly consistent with this interpretation. They reported that thin toluene films deposited near 0.85 T_g showed high kinetic stability and that the onset temperature during temperature scanning increased with film thickness up to 50 nm. They also concluded that a surface-initiated transformation mechanism was likely responsible for this behavior. The difference between the ~ 50 nm crossover distance for toluene and the ~ 1 μm crossover for IMC might be related to the very high temperature scanning rate utilized in reference 45.

Figure 7 illustrates that the transformation time becomes nearly constant for films thicker than 1 μm, suggesting a distinct bulk transformation mechanism as discussed previously.[28] For the thinnest films, the packing is so efficient that no molecular rearrangement occurs in the interior of the sample before the surface-initiated growth front has moved through the film. For the thickest films, imperfections in the low energy amorphous packing in the interior of the stable glass allow the transformation into the supercooled liquid before the front has propagated through the entire sample.[28,54] For intermediate film thickness, both surface-initiated and bulk transformation events contribute significantly to the overall transformation kinetics.

The 1 μm length scale in Figure 7 has been previously interpreted as the length scale between transformation initiation sites in the bulk of the stable glass.[28] We imagine that once a region of supercooled liquid begins to grow in the middle of a sample, its radius increases linearly in time with the same growth rate described above. If this 1 μm length scale is structural in origin, then it should not change with T_{anneal}. This is indeed the case in Figure 7. Other arguments supporting this interpretation are given in reference 28.

Finally, it should be noted that the transformation kinetics are much slower than the structural relaxation time τ_α of the supercooled liquid at T_{anneal} regardless of sample thickness or transformation mechanism. τ_α for IMC at a T_{anneal} of 320 K is about 10 seconds based on dielectric relaxation studies.[29,30] The transformation times reported here are 10^2 to $10^{3.5}$ times longer than τ_α depending on T_{anneal} and sample thickness; these tranformation times are much longer than what is observed for highly aged glasses formed by cooling the supercooled liquid.[55]

qi-TMDSC vs. nanocalorimetry. For the thickest films shown in Figure 7, conventional qi-TMDSC was used to obtain the isothermal transformation times. As illustrated in Figure 10, the shapes of $\phi_{SG}(t)$ for the qi-TMDSC data[16] and the thickest nanocalorimetry films (2.9 μm) are significantly different even though the transformation times are very similar. Deposition conditions were the same for both experiments with $T_{substrate}$ = 265 K and a deposition rate of 0.2 nm/s. For the ~30 μm thick glass studied with conventional qi-TMDSC, a gradual decrease in ϕ_{SG} is observed at early times. After about 15,000 seconds, the transformation into the supercooled liquid happens more quickly, as shown by the steeper slope for $\phi_{SG}(t)$. This change in slope nearly coincides with the peak in ϕ_{SG} for the 2.9 μm thick film at intermediate transformation times.

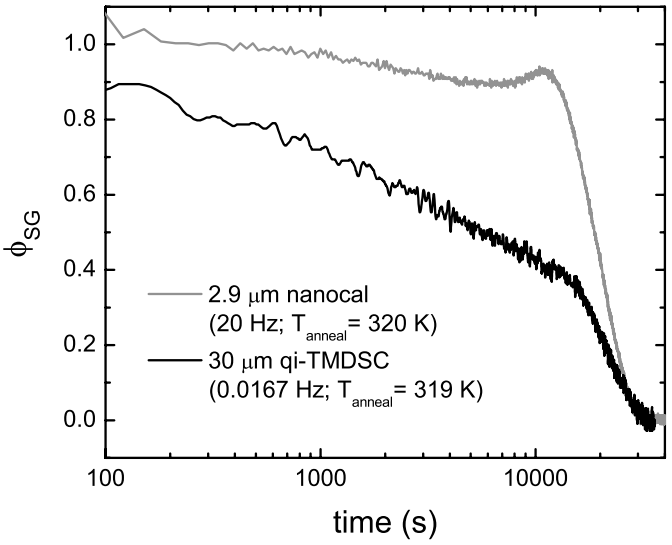

Figure 10: Comparison of $\phi_{SG}(t)$ obtained from different quasi-isothermal calorimetric techniques. AC nanocalorimetry was used for the 2.9 μm thick sample (gray) while conventional qi-TMDSC was used for the 30 μm sample (black).

The origin of the differing shapes of $\phi_{SG}(t)$ for the 2.9 μm and 30 μm thick films in Figure 10 has yet to be pinpointed. Given the control experiments in Figure 5 and 6 for the 2.9 μm thick films,

the discrepancies in shape are not due to T_{anneal} or the frequency or amplitude of the temperature oscillation. Similar controls have been performed for the qi-TMDSC experiments. In future work, it may be possible to extend the nanocalorimetry experiments to thicker films.

Thickness dependence of τ_α. In the last 15 years, significant efforts have been made to understand how T_g depends upon the thickness of a polymer film. Ellipsometry studies on supported films of polystyrene going back to 1994 [56] have been interpreted to indicate that the T_g decreases by tens of degrees for films less than 30 nm thick.[57,58] This depression of T_g is often described in terms of enhanced dynamics at the surface of the polymer films.[41,43,59] Dielectric relaxation measurements have also been utilized to interrogate the dynamics in thin polymer films. To date, some studies have found faster dynamics in thin films while others have reported essentially no changes. [60-62]

In contrast to the ellipsometric studies, nanocalorimetry studies of thin polymer films have yet to observe a thickness dependence in T_g[18,19,22] or, for the case of AC nanocalorimetry, τ_α.[18,23] Allen and coworkers first studied thin films of polystyrene with nanocalorimetry for thicknesses down to 1.4 nm.[22] An appreciable shift in T_g was not observed as a function of thickness. Schick and co-workers, using AC nanocalorimetry, have similarly observed a similar thickness independent τ_α for polystyrene[18] and poly(2,6-dimethyl-1,5-phenylene oxide) films.[23]

The τ_α data in Figure 9 obtained from AC nanocalorimetry for the supercooled liquid of IMC shows thickness-independent dynamics for films between 300 nm and 2900 nm. For these films, the τ_α obtained here from AC nanocalorimetry is in reasonable agreement with previous

dielectric relaxation studies performed on bulk IMC.[29,30] A slight shift to lower temperature is observed for the 150 nm thick films. Nonetheless, this temperature shift is much smaller than the T_g shifts discussed above. Since the thickness of the enhanced surface layer in IMC is estimated to be only a few nm thick,[13] it is expected that the average dynamics of a 150 nm film are nearly bulk-like. If dewetting can be overcome, the extension of these measurements on IMC to thinner films would be very interesting.

Summary

Glasses of indomethacin were vapor-deposited directly onto nanocalorimeter membranes and the reversing heat capacity was measured in range of 20-200 Hz. We find that for $T_{substrate}$ = 265 K, the molar heat capacity of the as-deposited glass is approximately 19 J/(mol K) lower than either the ordinary glass prepared by cooling the supercooled liquid or the glass prepared by vapor deposition at a $T_{substrate}$ = 315 K. This heat capacity difference is much larger than what has been previously observed between aged and ordinary glasses. Using this effect, we were able to observe the time evolution of the heat capacity as the stable glass transformed into the supercooled liquid. For films thinner than 1μm, the time to transform the film increased linearly with film thickness. For thick films, the transformation time was independent of film thickness. These results are consistent with two transformation mechanisms that occur in parallel. A surface-initiated growth front is the dominant transformation mechanism for thin films. For thick films, a bulk mechanism involving radially propogating fronts is postulated. Finally,

essentially no thickness dependence of the structural relaxation time τ_α was shown for the supercooled liquid of IMC.

Acknowledgements

We gratefully acknowledge joint funding from the U.S. National Science Foundation and the German Science Foundation (CHE-0724062 and DFG-SCHI 331 14-1, respectively). KLK KW and MDE also acknowledge additional funding from the National Science Foundation (CHE-0605136).

References

(1) Ishii, K.; Nakayama, H.; Okamura, T.; Yamamoto, M.; Hosokawa, T., J. Phys. Chem. B **107**, 876, (2003).

(2) Takeda, K.; Yamamuro, O.; Suga, H., J. Phys. Chem. **99**, 1602, (1995).

(3) Djurisic, A. B.; Kwong, C. Y.; Guo, W. L.; Lau, T. W.; Li, E. H.; Liu, Z. T.; Kwok, H. S.; Lam, L. S. M.; Chan, W. K., Thin Solid Films **416**, 233, (2002).

(4) Kwong, C. Y.; Djurisic, A. B.; Roy, V. L.; Lai, P.; Chan, W. K., Thin Solid Films **458**, 281, (2004).

(5) Greer, A. L., Science **267**, 1947, (1995).

(6) Hellman, F., Appl. Phys. Lett. **64**, 1947, (1994).

(7) Smith, R. S.; Kay, B. D., Nature **398**, 788, (1999).

(8) Stevenson, K. P.; Kimmel, G. A.; Dohnalek, Z.; Smith, R. S.; Kay, B. D., Science **283**, 1505, (1999).

(9) Turnbull, D., Metall. Mater. Trans. A **12**, 695, (1981).

(10) Oguni, M.; Hikawa, H.; Suga, H., Thermochim. Acta **158**, 143, (1990).

(11) Takeda, K.; Yamamuro, O.; Oguni, M.; Suga, H., Thermochim. Acta **253**, 201, (1995).

(12) Kearns, K. L.; Swallen, S. F.; Ediger, M. D.; Wu, T.; Yu, L., J. Chem. Phys. **127**, 154702, (2007).

(13) Swallen, S. F.; Kearns, K. L.; Mapes, M. K.; Kim, Y. S.; McMahon, R. J.; Ediger, M. D.; Wu, T.; Yu, L.; Satija, S., Science **315**, 353, (2007).

(14) Swallen, S. F.; Kearns, K. L.; Satija, S.; Traynor, K.; McMahon, R. J.; Ediger, M. D., J. Chem. Phys. **128**, 214514, (2008).

(15) Kearns, K. L.; Swallen, S. F.; Ediger, M. D.; Wu, T.; Sun, Y.; Yu, L., J. Phys. Chem. B **112**, 4934, (2008).

(16) Kearns, K. L.; Sun, Y.; Swallen, S. F.; Yu, L.; Ediger, M. D., J. Phys. Chem. B **113**, 1579, (2009).

(17) Efremov, M. Y.; Olson, E. A.; Zhang, M.; Schiettekatte, F.; Zhang, Z. S.; Allen, L. H., Rev. Sci. Inst. **75**, 179, (2004).

(18) Huth, H.; Minakov, A. A.; Schick, C., J. Poly. Sci. Pt. B-Poly. Phys. **44**, 2996, (2006).

(19) Leon-Gutierrez, E.; Garcia, G.; Lopeandia, A. F.; Fraxedas, J.; Clavaguera-Mora, M. T.; Rodriguez-Viejo, J., J. Chem. Phys. **129**, 181101, (2008).

(20) Queen, D. R.; Hellman, F., Rev. Sci. Instrum. **80**, 063901, (2009).

(21) Lai, S. L.; Carlsson, J. R. A.; Allen, L. H., Appl. Phys. Lett. **72**, 1098, (1998).

(22) Efremov, M. Y.; Olson, E. A.; Zhang, M.; Zhang, Z.; Allen, L. H., Phys. Rev. Lett. **91**, 085703, (2003).

(23) Zhou, D.; Huth, H.; Gao, Y.; Xue, G.; Schick, C., Macromolecules **41**, 7662, (2008).

(24) Chang, S. S.; Bestul, A. B., J. Res. Nat. Bureau Std. Sec. A **A 75**, 113, (1971).

(25) Chang, S. S.; Bestul, A. B., J. Chem. Phys. **56**, 503, (1972).

(26) Chang, S. S.; Bestul, A. B., J. Chem. Thermo. **6**, 325, (1974).

(27) Chang, S. S.; Horman, J. A.; Bestul, A. B., J. Res. Nat. Bureau Std. Sec. A **A 71**, 293, (1967).
(28) Kearns, K. L.; Huth, H.; Schick, C.; Ediger, M. D., J. Phys. Chem. Lett. **1**, 388, (2010).
(29) Carpentier, L.; Decressain, R.; Desprez, S.; Descamps, M., J. Phys. Chem. B **110**, 457, (2006).
(30) Wojnarowska, Z.; Adrjanowicz, K.; Wlodarczyk, P.; Kaminska, E.; Kaminski, K.; Grzybowska, K.; Wrzalik, R.; Paluch, M.; Ngai, K. L., J. Phys. Chem. B **113**, 12536, (2009).
(31) Weyer, S.; Huth, H.; Schick, C., Polymer **46**, 12240, (2005).
(32) Minakov, A. A.; Adamovsky, S. A.; Schick, C., Thermochim. Acta **432**, 177, (2005).
(33) Dawson, K. J.; Kearns, K. L.; Ediger, M. D.; Sacchetti, M. J.; Zografi, G. D., J. Phys. Chem. B **113**, 2422, (2009).
(34) Kearns, K. L.; Still, T.; Fytas, G.; Ediger, M. D., Adv. Mat. **22**, 39, (2010).
(35) Swallen, S. F.; Traynor, K.; McMahon, R. J.; Ediger, M. D.; Mates, T. E., Phys. Rev. Lett. **102**, 065503, (2009).
(36) Swallen, S. F.; Windsor, K.; McMahon, R. J.; Ediger, M. D.; Mates, T. E., J. Phys. Chem. B, (accepted).
(37) Damman, P.; Baudelet, N.; Reiter, G., Phys. Rev. Lett. **91**, 216101, (2003).
(38) Hensel, A.; Dobbertin, J.; Schawe, J. E. K.; Boller, A.; Schick, C., J. Therm. Anal. **46**, 935, (1996).
(39) Alcoutlabi, M.; McKenna, G. B., J. Phys.: Condens. Matter **17**, R461, (2005).
(40) Bell, R. C.; Wang, H. F.; Iedema, M. J.; Cowin, J. P., J. Am. Chem. Soc. **125**, 5176, (2003).
(41) Ellison, C. J.; Torkelson, J. M., Nat. Mater. **2**, 695, (2003).
(42) Forrest, J. A.; Dalnoki-Veress, K., Adv. Colloid Interface Sci. **94**, 167, (2001).
(43) Fakhraai, Z.; Forrest, J. A., Science **319**, 600, (2008).
(44) Dawson, K. J.; Kearns, K. L.; Yu, L.; Steffen, W.; Ediger, M. D., Proc. Natl. Acad. Sci. U. S. A. **106**, 15165, (2009).
(45) Leon-Gutierrez, E.; Garcia, G.; Lopeandia, A. F.; Clavaguera-Mora, M. T.; Rodriguez-Viejo, J., J. Phys. Chem. Lett. **1**, 341, (2010).
(46) Ishii, K.; Nakayama, H.; Moriyama, R.; Yokoyama, Y., Bull. Chem. Soc. Jpn. **82**, 1240, (2009).
(47) Ishii, K.; Nakayama, H.; Hirabayashi, S.; Moriyama, R., Chem. Phys. Lett. **459**, 109, (2008).
(48) Shamblin, S. L.; Tang, X. L.; Chang, L. Q.; Hancock, B. C.; Pikal, M. J., J. Phys. Chem. B **103**, 4113, (1999).
(49) Guttman, C. M., J. Chem. Phys. **56**, 627, (1972).
(50) Moynihan, C. T.; Easteal, A. J.; DeBolt, M. A.; Tucker, J., J. Am. Ceram. Soc. **59**, 12, (1976).
(51) Narayanaswamy, O. S., J. Am. Ceram. Soc. **54**, 491, (1971).
(52) Tool, A. Q., J. Am. Ceram. Soc. **31**, 177, (1948).
(53) Angell, C. A.; Ngai, K. L.; McKenna, G. B.; McMillan, P. F.; Martin, S. W., J. Appl. Phys. **88**, 3113, (2000).
(54) Wolynes, P. G., Proc. Nat. Acad. Sci. USA **106**, 1353, (2009).
(55) Kovacs, A. J., Fortschr Hochpolym-Forsch. **3**, 394, (1963).

(56) Keddie, J. L.; Jones, R. A. L.; Cory, R. A., Europhys. Lett. **27**, 59, (1994).
(57) Kawana, S.; Jones, R. A. L., Phys. Rev. E **6302**, 021501, (2001).
(58) Roth, C. B.; Dutcher, J. R., Journal of Electroanalytical Chemistry **584**, 13, (2005).
(59) O'Connell, P. A.; Hutcheson, S. A.; McKenna, G. B., J. Poly. Sci. Part B-Poly. Phys. **46**, 1952, (2008).
(60) Fukao, K.; Miyamoto, Y., Phys. Rev. E **61**, 1743, (2000).
(61) Rotella, C.; Napolitano, S.; Wuebbenhorst, M., Macromolecules **42**, 1415, (2009).
(62) Serghei, A.; Huth, H.; Schick, C.; Kremer, F., Macromolecules **41**, 3636, (2008).